

## Conformation-Activity Relationship of Sweet Molecules. Comparison of Aspartame and Naphthimidazolesulfonic Acids

M. A. Castiglione-Morelli,<sup>||</sup> F. Lejl,<sup>†</sup> F. Naider,<sup>‡</sup> M. Tallon,<sup>‡</sup> T. Tancredi,<sup>§</sup> and P. A. Temussi<sup>\*,||</sup>

Dipartimento di Chimica, Università della Basilicata, Potenza, Italy, Department of Chemistry, St. George Campus, College of Staten Island, City University of New York, Staten Island, New York 10301, Istituto Chimica MIB del CNR, via Toiano 6, Arco Felice, Napoli, Italy, and Dipartimento di Chimica, Università di Napoli, via Mezzocannone 4, 80134 Napoli, Italy.  
Received January 30, 1989

The shape of the active site of the receptor for sweet molecules was previously defined on the basis of a combination of both rigid (saccharins) and flexible (aspartame) molds. In this paper, the sweetness receptor is refined with use of the shapes of 3-anilino-2-styryl-3*H*-naphtho[1,2-*d*]imidazolesulfonate (sweet) and of 3-anilino-2-phenyl-3*H*-naphtho[1,2-*d*]imidazolesulfonate (tasteless), two large and almost completely rigid tastants. The minimum-energy conformations of the flexible portions of these tastants have been determined by using a detailed conformational analysis based on *ab initio* calculations. The refined receptor site is still consistent with all previously examined sweet molecules. In order to unequivocally assign the prochiral  $\beta$ -CH<sub>2</sub> protons of the Phe moiety of aspartame, (2*S*,3*S*)-[<sup>2</sup>H]- $\alpha$ -L-Asp-L-PheOMe was synthesized and examined by 500-MHz <sup>1</sup>H NMR spectroscopy. The results indicate that the minimum-energy conformation for aspartame in water, DMSO-*d*<sub>6</sub>, and CDCl<sub>3</sub> (as a crown ether complex) is different from that originally proposed (F<sub>II</sub>D<sub>II</sub> instead of F<sub>I</sub>D<sub>II</sub>, according to a notation referred to the side chains). Although this conformation is not directly consistent with the shape of the sweet receptor, the interconversion of F<sub>II</sub>D<sub>II</sub> to F<sub>I</sub>D<sub>II</sub> was found to require only 1 kcal/mol. Furthermore, a 120-ps molecular dynamics simulation in vacuo confirms the high flexibility of aspartame and the accessibility of the F<sub>I</sub>D<sub>II</sub> conformer whose topology is fully consistent with our model.

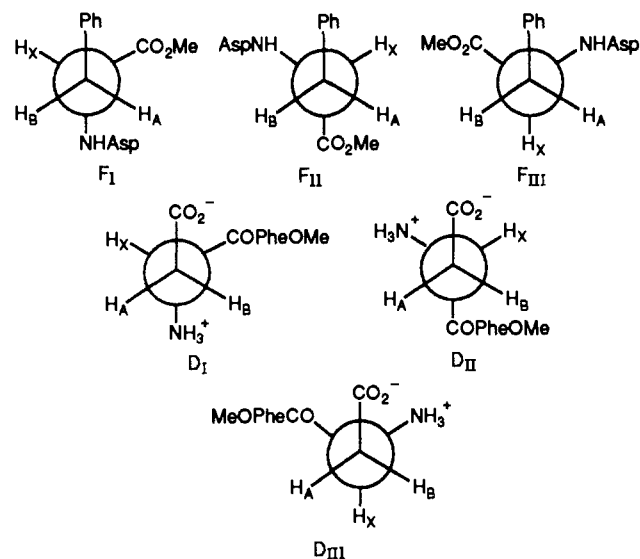
Sweetness is a stimulus of the peripheral nervous system imparted by a very large number of molecules of widely different chemical nature.<sup>1</sup> The ready availability of many agonists and the practical importance of sweeteners has always stimulated the search for unifying features among the known sweet molecules and/or for general models of the active site of the receptor protein.<sup>2-9</sup> The first structural (and electronic) feature identified in most sweet molecules is the so-called AH-B entity.<sup>3</sup> Shallenberger and Acree pointed out that nearly all sweet molecules have a hydrogen bond donor (AH) and a hydrogen bond acceptor (B) separated by ca. 0.3 nm. These groups are thought to form two hydrogen bonds with a complementary entity present in the active site of the receptor.

Later we were able to show that the AH-B entity could be incorporated in a much more general model of receptor site.<sup>5</sup> The main features of our model can be summarized as follows. (i) The active site of the receptor is a shallow, flat cavity with the outer side accessible even during the interaction with the agonist.<sup>5a,d</sup> (ii) The lower part of the cavity contains the main "electronic features", the most important of these being the AH-B entity; this part is always essential for the binding. (iii) The upper part is hydrophobic and plays an important role in the case of very active tastants.

Figure 1 shows the contour of the model site in two dimensions, together with the twin model for the bitter receptor. The two-dimensional representation was not chosen owing to its obvious simplicity but because it reflects an actual property of our model; i.e. in our vision the active site is a very shallow cavity, nearly two-dimensional owing to the peculiar symmetry relationship existing between the sweet and bitter receptor sites.<sup>5</sup>

That is, a simple way of explaining the change of taste (from sweet to bitter) of simple amino acids upon changing their chirality is to hypothesize two very similar, flat active sites in which only the AH-B entities are reversed (i.e. a C<sub>2</sub> operation). The shape of the lower part, drawn with a solid line in Figure 1, was determined rather accurately

Chart I



with the aid of several "molecular molds", i.e. by comparing the shapes of many rigid and very sweet molecules, all with a consistent orientation of their AH-B entity.<sup>5a</sup> The shape

<sup>†</sup> Università della Basilicata, Potenza, Italy.

<sup>‡</sup> Department of Chemistry, City University of New York, New York.

<sup>§</sup> Istituto Chimica MIB del CNR, Arco Felice, Italy.

<sup>||</sup> Università di Napoli, Napoli, Italy.

(1) Moncrieff, R. W. *The Chemical Senses*; Hill: London, 1967.

(2) Cohn, G. *Die Organischen Geschmackstoffe*; Siemuroth: Berlin, 1914.

(3) (a) Shallenberger, R. S.; Acree, T. *Nature (London)* **1967**, *216*, 480-482. (b) Shallenberger, R. S.; Acree, T.; Lee, C. Y. *Nature (London)* **1969**, *221*, 555-556.

(4) Kier, L. B. *J. Pharm. Sci.* **1972**, *61*, 1394-1397.

(5) (a) Temussi, P. A.; Lejl, F.; Tancredi, T. *J. Med. Chem.* **1978**, *21*, 1154-1158. (b) Tancredi, T.; Lejl, F.; Temussi, P. A. *Chem. Senses Flavor* **1979**, *4*, 259-264. (c) Ciajolo, M. R.; Lejl, F.; Tancredi, T.; Temussi, P. A.; Tuzl, A. *J. Med. Chem.* **1983**, *26*, 1060-1064. (d) Temussi, P. A.; Lejl, F.; Tancredi, T.; Castiglione-Morelli, M. A.; Pastore, A. *Int. J. Quantum Chem.* **1984**, *26*, 889-906.

(6) (a) Mazur, R. H.; Schlatter, J. M.; Goldkamp, A. H. *J. Am. Chem. Soc.* **1969**, *91*, 2684-2691. (b) van der Heljden, A.; Brussel, L. B. P.; Peer, H. G. *Food Chem.* **1978**, *3*, 207-213.

(7) Iwamura, H. *J. Med. Chem.* **1981**, *24*, 572-578.

(8) Goodman, M.; Coddington, J.; Mierke, D. F. *J. Am. Chem. Soc.* **1987**, *109*, 4712-4714.

(9) Walters, D. E.; Pearlstein, R. A.; Krimmel, C. P. *J. Chem. Educ.* **1986**, *63*, 869-871.

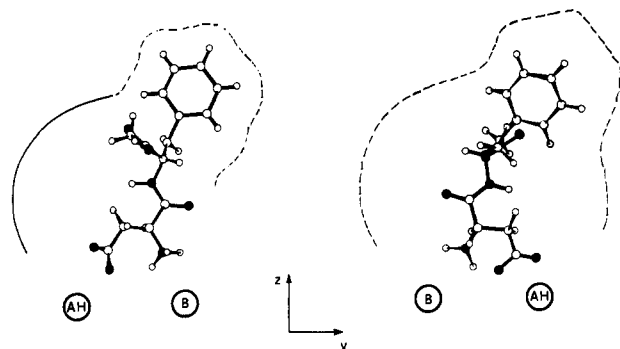


**Figure 1.** Schematic representation of sweet (left) and bitter (right) site models, as derived from ref 5a-d. The view corresponds to a section of the sites in the  $yz$  plane, containing the AH-B entities.<sup>3</sup> The  $+x$  direction corresponds to the open outer side of the sites. The molecular models allocated in the sites are two of the more populated conformers of respectively the sweet  $\alpha$ -L-Asp-L-PheOMe and the bitter  $\alpha$ -D-Asp-D-PheOMe dipeptides.

of the upper part, drawn with a dashed line in Figure 1, was originally based on the most probable solution conformation of aspartame<sup>5a,10</sup> but received further confirmation by the rationalization of the taste properties of nonpeptidic sweet molecules.<sup>5</sup>

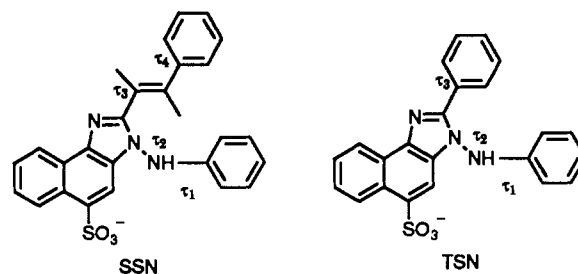
A recent comparison<sup>9</sup> of the shapes of three-dimensional receptor models has shown that our model had more heuristic power than others. This was in spite of the fact that its reproduction by the quoted authors<sup>9</sup> was not completely faithful (i.e. the open part of the cavity had been exchanged with the flat bottom).

At any rate, our model cannot be considered a complete geometrical model but rather a topological model, since only rigid molecules are fully reliable as molds. In addition, it has recently been pointed out<sup>11</sup> that the original assignment of the prochiral  $\beta$ -CH<sub>2</sub> protons of Phe in aspartame<sup>10</sup> might be erroneous. This assignment was previously used to help delineate the upper part of the model of Figure 1, whose shape corresponds to rotamer F<sub>II</sub>D<sub>II</sub> (see Chart I). Thus, as hinted by the authors of ref 11, one should consider rotamer F<sub>II</sub>D<sub>II</sub> in the analysis of the receptor binding site, but one should also take into account the F<sub>III</sub>D<sub>II</sub> conformation found in the solid state,<sup>12</sup> even though it is less favored on the basis of solution NMR studies. On the basis of these conclusions, we have chosen to reexamine the solution conformation of aspartame, using a combination of stereospecific  $\beta$ -deuteration, NMR analysis, and energy calculations.

Regardless of the results with aspartame, however, our model is not based completely on a study of this tastant. Firstly, we did not simply rely on "the minimum-energy conformation" to delineate the shape of the model.<sup>10</sup> Rather we examined all conformations near the energy that were suggested by both NMR and theoretical studies.<sup>10</sup> Thus the shape of the upper part of the model was based both on the conformation of aspartame and more general considerations.

It is the purpose of this paper to revise the conformation of aspartame and to transform the active-site model into a detailed geometrical model. We approach this latter objective by examining increasingly larger and more rigid molds. In this context we sought a class of very large, flat, and rigid tastants.

**Chart II**



Among the largest known sweet molecules are the sulfonaphthoimidazoles resulting from the condensation of 1-amino-2-phenylazonaphthalene-4-sulfonic acid with various aldehydes.<sup>13</sup>

Here we report a conformational analysis of two such compounds: the very sweet 3-anilino-2-styryl-3H-naphtho[1,2-d]imidazole-5-sulfonate, a sweet sulfonaphthoimidazole (henceforth called SSN; Chart II) and the tasteless analogue 3-anilino-2-phenyl-3H-naphtho[1,2-d]imidazole-5-sulfonate (henceforth called TSN).

## Results and Discussion

**Conformational Analysis of Sulfonaphthoimidazoles.** Originally, sulfonaphthoimidazoles were described as sulfonaphthotriazines,<sup>13</sup> but an X-ray diffraction study<sup>14a</sup> of TSN showed its correct molecular skeleton. Crystallization of SSN was not successful, but it was possible to prove its constitution with the aid of NMR spectroscopy.<sup>14b</sup>

The proton and carbon spectra of TSN are fully consistent with the molecular model derived from the X-ray analysis, and application of several 1-D and 2-D techniques led to a complete assignment of all resonances.<sup>14b</sup> A comparison with the analogous spectra of SSN confirmed that the only difference between the two compounds resides in the presence of a trans double bond between the carbon atom of the imidazole ring and the phenyl group.<sup>14b</sup>

Thus it is possible to build molecular models of both compounds on the basis of the solid-state parameters of TSN. However, before using either model as a molecular mold, it is necessary to perform a detailed analysis to determine the conformational preferences around the single bonds.

The naphthoimidazole skeleton is extremely rigid; therefore it is possible to assess the conformational preferences by simple empirical calculations of the internal energy as a function of a maximum of four internal rotation angles (indicated with symbols  $\tau_1$  to  $\tau_4$  in Chart II). Conformational energy calculations were based mainly on pairwise summation over all van der Waals interactions according to eq 1, where  $E_{nb}$  is the energy due to inter-

$$E_{\text{conf}} = E_{\text{nb}} + \sum_i V_{0,i} \sin^2 \tau_i \quad (1)$$

actions between atoms separated by more than two bonds; the second term is an intrinsic torsional potential that takes into account conjugative interactions<sup>15</sup> relative to the  $i$ th bond.

Minimum-energy conformations for TSN and SSN have been searched by using the Davidon-Fletcher-Powell<sup>16</sup> and Newton-Raphson<sup>17</sup> algorithms in connection with ana-

(10) Lelej, F.; Tancredi, T.; Temussi, P. A.; Tonolo, C. *J. Am. Chem. Soc.* **1976**, *98*, 6669-6674.

(11) Slemion, I. Z.; Picur, B. *Pol. J. Chem.* **1984**, *58*, 475-478.

(12) Hatada, M.; Jancarlik, J.; Graves, B.; Kim, S. *J. Am. Chem. Soc.* **1985**, *107*, 4279-4282.

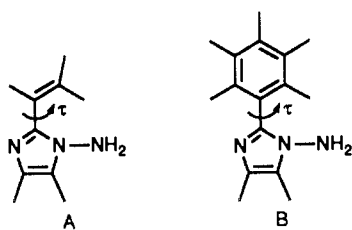
(13) Neri, A. *Gazzetta* **1941**, *71*, 201-214.

(14) (a) Clajolo, M. R.; Parrilli, M.; Temussi, P. A.; Tuzi, A. *Acta Crystallogr.* **1983**, *C39*, 983-984. (b) Parrilli, M.; Pastore, A.; Temussi, P. A. *Magn. Reson. Chem.* **1986**, *1*, 1-3.

(15) Fischer-Hjalmars, I. *Tetrahedron* **1963**, *19*, 1805-1810.

(16) (a) Fletcher, R.; Powell, M. J. D. *Comput. J.* **1963**, *6*, 163-167. (b) Davidon, W. C. *Computer J.* **1963**, *10*, 406-410.

Chart III



lytical computation of first and second derivatives of eq 1. X-ray geometries have been used for TSN and the common part of SSN. In the latter case the geometry of the styryl moiety has been chosen according to standard geometrical data. The force field employed in the calculations based on eq 1 was selected among several force fields proposed in the literature.<sup>18-21</sup>

The final results reported in this paper were obtained by using the parameters for nonbonded atom interactions proposed by Burkert and Allinger.<sup>19</sup> Unfortunately, only the value of  $V_0$  corresponding to  $\tau_4$  can be found in this force field, for bonds involved in conjugative interactions.

Owing to the somewhat unusual skeleton of TSN and SSN, the choice of literature values for  $V_0$  for other  $\tau$ 's is rather limited and there is complete lack of experimental data about the barriers for the molecules under study.

On the other hand, the  $V_0$  term in eq 1 is mandatory to reproduce correctly the torsional behavior around  $\tau$  angles, owing to the presence of  $\pi$  systems in the two moieties of the molecule. Even at the minimum basis set level (a forced choice when dealing with very large molecules), ab initio calculations are able to reproduce the conformational behavior of conjugated molecules both qualitatively and quantitatively.<sup>22</sup> Thus such calculations avoid the pitfalls of semiempirical methods such as CNDO or MNDO.

The extremely large number of non-hydrogen atoms in TSN and SSN makes the use of ab initio computations rather arduous, even at the minimum basis set level. Therefore we have performed the ab initio computations using the model compounds A and B (shown in Chart III) which retain most of the important features influencing the  $\tau_4$  barrier, yet allow a strong reduction in the number of base functions. Ab initio computations were performed by means of the GAUSSIAN-80 set of programs<sup>23</sup> at the STO-3G level. The conformational behavior of the model compounds A and B at the ab initio level was examined by scanning the angle  $\tau$  in steps of 30°. The imidazole ring was fixed at its experimental geometry<sup>14a</sup> whereas the phenyl ring and the ethylene moieties have been assumed in their standard geometries, that is, 120° for all valence angles, 1.39 and 1.08 Å for C-C and C-H bond distances in the case of phenyl, and 1.33 and 1.08 Å for C-C and C-H bond distances for the ethylene moiety. Table IA,B summarizes the internal energy values as a function of the

**Table I.** Comparison of Computed Energies (kcal/mol) for the Scheme III Model Compounds A and B, According to Ab Initio and Empirical Computations

compd	$\tau$ , deg	ab initio	Hopfinger	Allinger
A	0	0.00	0.00	0.00
	30	1.47	1.49	1.62
	60	4.89	5.10	5.00
	90	6.91	6.20	6.90
	120	5.38	5.10	5.13
	150	2.70	2.58	2.23
	180	2.16	3.60	2.25
B	0	0.00	0.00	0.00
	30	0.93	-1.93	-0.76
	60	3.90	2.41	3.07
	90	5.71	5.71	5.71

relevant torsion (shown in Chart III) for model compounds A and B, respectively.

In order to extract the values of  $V_0$ , the ab initio conformational energies have been fitted with use of eq 1, since it has been shown<sup>15</sup> that conjugative contributions can be easily reproduced by the second term of eq 1. Besides, in the case of  $E_{nb}$  several empirical functions and parameters have been developed and applied to different systems.<sup>18-21</sup> We have used (i) the R6-R12 functional expression together with the Hopfinger parametrization<sup>18</sup> and (ii) the Allinger parametrization<sup>19</sup> and an EXP-R6 type of functional expression. The two parameter sets have been used in connection with eq 1, and different values of  $V_0$  have been tried in order to reproduce the energies computed at ab initio level (Table IA). For compound A the  $V_0$  values which give the best fit of the ab initio energies amount to 9.5 and 7.6 kcal/mol for the Hopfinger R6-R12 and the Allinger EXP-R6 parametrization, respectively. Table I shows that the Hopfinger parametrization is unable to give a good fit of the ab initio energies. In fact, both the barrier (6.20 versus 6.91 kcal/mol) at 90° and the energy difference between 0° and 180° (3.60 versus 2.16 kcal/mol) are badly reproduced by this parametrization.

The Allinger parametrization allows a better fitting of both the 90° barrier (6.90 versus 6.91 kcal/mol) and the 0-180° energy difference (2.25 versus 2.16 kcal/mol). Furthermore, the intrinsic torsional potential ( $V_0$ ) obtained by using the Allinger parametrization compares well with those relative to a series of vinyl pyridines<sup>24</sup> and to styrene<sup>25</sup> which shows an intrinsic potential  $V_0$  of 6.0 kcal/mol. These results are also in agreement with the value of 7.0 kcal/mol suggested by Hummel and Flory.<sup>26</sup> The analogous approach in the case of B suggests a  $V_0$  of 8.27 and 5.77 kcal/mol respectively for Hopfinger and Allinger parametrizations.

The values of  $V_0$  obtained for model compounds A and B have then been transferred to SSN and TSN in order to search for minimum-energy conformations in the  $\tau_1$ ,  $\tau_2$ ,  $\tau_3$ ,  $\tau_4$  conformational space. In the case of TSN we have minimized the conformational energy starting from a total of 45 conformations, obtained by combinations of three conformations relative to  $\tau_1$  (80°, 90°, and 100°), three conformations relative to  $\tau_2$  (-70°, -90°, and -100°), and finally five conformations relative to  $\tau_3$  (30°, -30°, 60°, -60°, and 90°). Only three minimum-energy conformations have been obtained; they are characterized by relative

- (17) Fletcher, R. VA011A subroutine, AERE Harwell Library.  
 (18) Hopfinger, A. J. *Conformational Properties of Macromolecules*; Academic Press: New York, 1963.  
 (19) Burkert, V.; Allinger, N. L. *Molecular Mechanics*; ACS Monograph 177; American Chemical Society: Washington, DC, 1982.  
 (20) Hagler, A. T.; Huler, E.; Lifson, S. *J. Am. Chem. Soc.* **1974**, *96*, 5319-5326.  
 (21) Oie, T.; Maggiora, G. M.; Christoffersen, R. E.; Duchamp, D. *J. Int. J. Quantum Chem., Quantum Biol. Symp.* **1981**, 1-47.  
 (22) Barone, V.; Lelj, F.; Cautletti, C.; Piancastelli, M. N.; Russo, N. *Mol. Phys.* **1983**, *49*, 599-619.  
 (23) Binkley, J. S.; Whiteside, R. A.; Krishnan, R.; Seeger, R.; DeFrees, D. J.; Schlegel, H. B.; Topiol, S.; Kahn, L. R.; Pople, J. A. *Quantum Chemistry Program Exchange* **1982**, No. 430.

- (24) Barone, V.; Bianchi, N.; Lelj, F.; Abbate, G.; Russo, N. *J. Mol. Struct. (THEOCHEM)* **1984**, *108*, 35-41.  
 (25) Almlof, J. E.; Isacsson, P. U.; Mjoberg, P. J.; Ralowski, W. *Chem. Phys. Lett.* **1974**, *26*, 215-217.  
 (26) Hummel, J. P.; Flory, P. J. *Macromolecules* **1980**, *13*, 479-484.

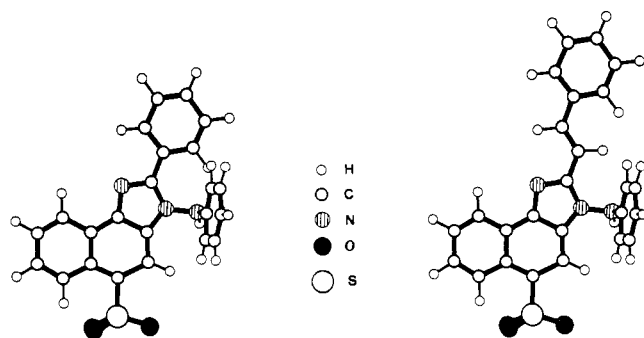


**Figure 2.** Molecular models of the minimum-energy conformations of TSN (left) and SSN (right), as derived from the conformational analysis.

energies of 0.00, 0.28, and 0.88 kcal/mol. The values of  $\tau_3$  and  $\tau_2$  in the minimum-energy conformation ( $-41.3^\circ$  and  $-79^\circ$ ) compare well with the values of  $-41^\circ$  and  $-75^\circ$  found in the solid state.<sup>14a</sup>

Several different starting conformations have been chosen in the case of SSN, but all of them collapse to a unique minimum characterized by the ethylenic double bond trans with respect to the anilino nitrogen. The other minimum, which can be observed in the case of model compound A, disappears due to the unfavorable interactions with the bulky phenyl group linked to the anilino nitrogen. In the minimum-energy conformation both the naphthoimidazole and the styryl moiety lie in the same plane, resulting in a very flat shape of the system connecting the naphthoimidazole ring and the styryl moiety. The equilibrium conformation of the anilino substituent is very similar to the corresponding moiety of TSN, being characterized by values of  $\tau_1$  and  $\tau_2$  of  $81^\circ$  and  $-92^\circ$ , respectively, i.e. almost exactly perpendicular to the plane of the naphthoimidazole moiety. The molecular models are shown in Figure 2.

It is necessary to point out that since the naphthoimidazole moiety is flat, the conformations characterized by a position of the anilino group above or below the plane of the molecule have the same energy if the torsion angles are chosen in a correct way. This feature is relevant since the single conformer observed in the solid state<sup>14a</sup> for TSN is not compatible with the receptor model. Its anilino group would in fact invade the wall that constitutes the bottom of the active site.<sup>3b</sup>

The active site of the sweet receptor is chiral and can accordingly select between the two enantiomeric conformations which can be obtained when the phenyl group of the anilino moiety is "above" or "below" the plane of the naphthoimidazole moiety.

**Refinement of the Model Site.** We can now use the shape of (very sweet) SSN, derived from the conformational analysis, to improve the model of Figure 1. That is, we can determine a more reliable contour of the upper part of the model, provided the shape of SSN is consistent with that of the lower part derived from substituted saccharines.<sup>5</sup> A crucial point in comparing different sweet molecules, and hence in using a model site, is the possibility of orienting their AH-B entities in the same way. This is not straightforward in the case of SSN (and TSN) since its AH-B entity is intrinsically different from those of most other sweet compounds. Strictly speaking, the anionic form has only the B part of the entity, i.e. the  $\text{SO}_3^-$  group. The acidic form (very unlikely, due to the extremely low  $\text{p}K_a$ ) would have both AH and B in the single  $\text{SO}_3\text{H}$  group, i.e. two of the oxygens, like the oxygens of the  $\text{SO}_2$  group of saccharin, as B and the OH group as AH (instead of the NH of saccharin).

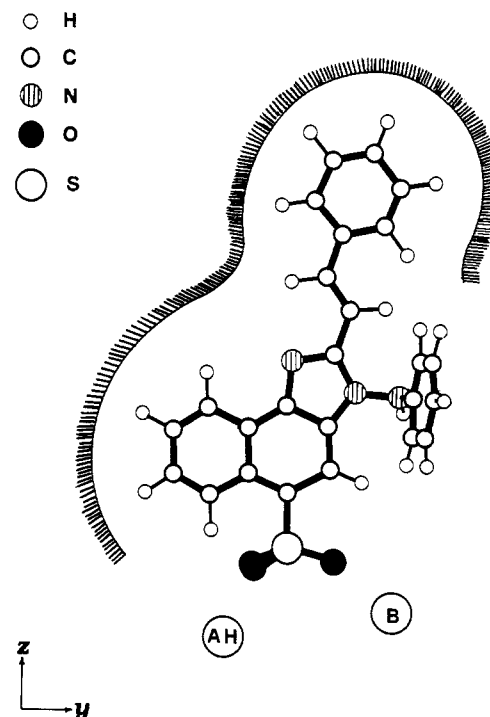


**Figure 3.** Section, along the  $yz$  plane containing the AH-B entities, showing the contour of the new site of the sweet taste, as derived from a combination of the mapping with saccharins<sup>5a</sup> and of the molecular model of SSN, shown in the site.

As a general rule, however, it is fair to say that an imperfect AH-B entity can well be tolerated by the site, provided the steric fit for the remainder of the molecule is very good.

This last requirement is certainly met by SSN and TSN since their sulfonaphthoimidazolyl moiety has a shape exactly complementary to the lower part of the model of Figure 1 and fills it completely. Actually, even the upper part of SSN (i.e. the styryl moiety) is very similar to that of the old model, only somewhat larger. It is important to emphasize that the styryl group is completely coplanar with the naphthoimidazole skeleton, thus assuring a very good hydrophobic interaction with the flat bottom of the site.

Figure 3 shows the contour of the new site, derived from a combination of the mapping with saccharins<sup>5a</sup> and of the molecular model of SSN. It is now possible to explain why the very similar molecule of TSN is tasteless. Figure 4 shows that when the phenyl ring is made coplanar with the naphthoimidazole skeleton (as suggested by the conformational analysis) a part of it overlaps with the right-hand side of the upper part of the contour. This interaction is bad enough to prevent a good fit by itself but, in addition, it is very critical for the fit of the complementary AH-B entities, since any rotation of the molecule in the  $yz$  plane would disalign the corresponding AH and B groups of the molecule and of the site. The modest tilt observed in the solid state and in some conformers with energies immediately higher than that of the absolute minimum is not sufficient to relieve this unfavorable interaction. On the other hand, any deviation from planarity sufficient to avoid the "invasion" of the right wall would lead to a very unfavorable interaction with the flat bottom of the site, the so-called barrier that, according to Shallenberger and Acree,<sup>3b</sup> prevents L-amino acids from fitting the sweet receptor site.

**Conformational Analysis of Aspartame.** The lowest energy conformation of aspartame derived in the quoted

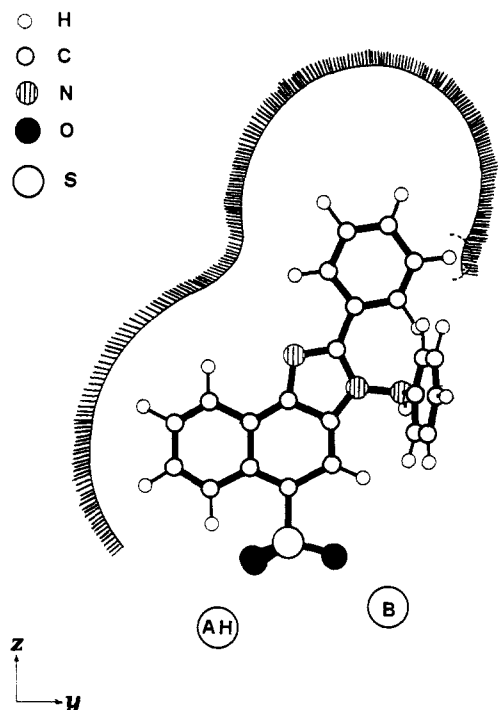


**Figure 4.** Representation of the bad fitting of TSN in the sweet site. The phenyl ring invades the right-hand side of the upper part of the site contour.

conformational analysis<sup>10</sup> is fully consistent with the revised model site depicted in Figure 3, a finding that is implied in the extreme similarity of the contours shown in Figures 1 and 3.

Once again we feel it necessary to emphasize that the shape of the site depicted in Figure 1 was only *indirectly* based on the conformation of aspartame in solution. In fact, in our original investigation we selected a few conformations of low internal energy and finally restricted the choice to the two of lowest energy ( $F_I D_{II}$  and  $F_{II} D_{II}$ ), characterized by almost identical backbone conformations but with a different conformation of the Phe side chain. Only one of these conformers ( $F_I D_{II}$ ) is fully consistent with the model site of Figure 3, since the ring of Phe is parallel to the A-B plane and does not invade the bottom wall of the site (the so-called Shallenberger barrier).

The other conformer ( $F_{II} D_{II}$ ) however can be converted into  $F_I D_{II}$  with a barrier of less than 1 kcal/mol, a modest value indeed, which can be easily compensated by the interaction with the receptor.

The identification of the two conformers of Figure 5 was based on a combination of NMR measurements and energy calculations.<sup>10</sup> A crucial point in the interpretation of the NMR data was the assignment of the prochiral  $\beta$ -CH<sub>2</sub> protons of Asp and Phe side chains. The high-field resonance of the Asp CH<sub>2</sub> was assigned to the *pro-R* proton as in all previous assignments for aspartic acid and Asp peptides.<sup>27</sup> The assignment of the Phe protons had to be reversed, with respect to literature data, to obtain consistency with energy calculations.<sup>10</sup>

However, our original assignment for Phe has been recently questioned,<sup>11</sup> since the aspartame analogue Asp-Met-OMe, selectively deuterated in the *pro-R*  $\beta$ -CH<sub>2</sub> proton of Met, showed an opposite assignment. On the other hand, a similar careful work on Phe derivatives<sup>28</sup> had

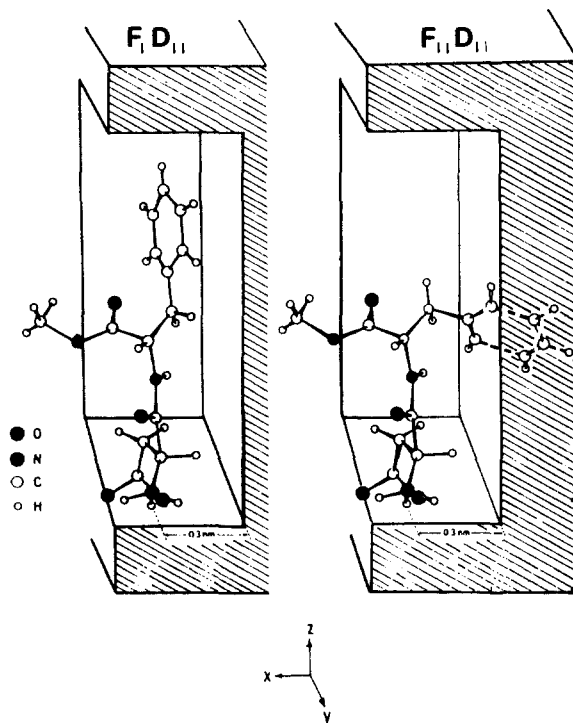


**Figure 5.** Schematic representation of the *xz* section of the sweet taste site, containing the two most populated conformers<sup>10</sup> of aspartame; in the  $F_{II} D_{II}$  conformer, the phenyl ring invades the bottom barrier of the site.

previously shown that the assignment can be a function of the environment. Thus the spectrum of *N*-acetylphenylalanine methylamide in polar solvents shows the resonance of *pro-R* at higher field than that of *pro-S*, but the relative positions are reversed when the same compound is dissolved in apolar solvents.

This observation seemed quite relevant in our case since both the energy calculations (in vacuo) and the in vivo interaction with the receptor can be likened to an apolar environment. Aspartame itself is nearly insoluble in apolar solvents but it is possible to dissolve it in CDCl<sub>3</sub> as a complex of 18-crown-6 ether.<sup>5d</sup> The combination of crown ether and apolar solvent mimics, in fact, two important features of the biological interaction, i.e. the binding of the charged groups (to a complementary AH-B entity of the receptor) and the prevailing hydrophobic environment of the active site. In the case of aspartame the crown ether binds strongly to the NH<sub>3</sub><sup>+</sup> group and forces the carboxyl group of the side chain into a *gauche* conformation<sup>5d</sup> as required by the minimum-energy global conformations.<sup>10</sup>

Accordingly we prepared a sample of aspartame selectively deuterated on the Phe side chain (see the Experimental Section) and recorded its <sup>1</sup>H NMR spectra in water, DMSO-*d*<sub>6</sub>, and CDCl<sub>3</sub> (as crown ether complex). The results are shown in Figure 6; it can be seen that the relative order of the two prochiral  $\beta$ -CH<sub>2</sub> protons remains the same in all environments studied and that the *pro-R* proton is at high field in agreement with the proposal by Feeney et al.<sup>27</sup> Therefore we must conclude that in solution, irrespective of the solvent, the most populated conformation is  $F_{II} D_{II}$ , and not  $F_I D_{II}$  as we originally proposed.<sup>10</sup> This finding, however, although of fundamental importance for an accurate description of the conformational preferences of aspartame in solution, is of minor relevance for the receptor model fitting. It is essential to recall that aspartame has considerable conformational flexibility; this circumstance makes pointless the search for a "lowest energy conformation", irrespective of the methods em-

(27) Feeney, J.; Roberts, G. C. K.; Brown, J. P.; Burgen, A. S. V.; Gregory, H. J. *J. Chem. Soc., Perkin Trans. 2* 1972, 2, 601-604.

(28) Kobayashi, J.; Nagai, U.; Higashijima, T.; Miyazawa, T. *Biochem. Biophys. Acta* 1979, 577, 195-206.

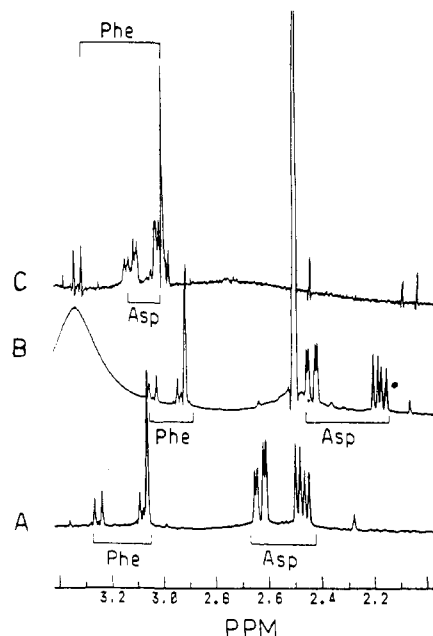


**Figure 6.** 500-MHz  $^1\text{H}$  NMR spectral region containing the prochiral  $\beta\text{-CH}_2$  resonances of (2S,3S)-[ $^2\text{H}$ ]-phenylalanyl aspartame in three different solvent systems: (A)  $\text{H}_2\text{O}$ , pH 8.9, (B)  $\text{DMSO-}d_6$ , and (C)  $\text{CDCl}_3/18\text{-crown-6}$  ether. All spectra have been run at 297 K and 1 mg/mL of deuterated aspartame. Chemical shifts are in ppm from tetramethylsilane.

ployed in the analysis. In fact, different environments favor different conformers: in several solution media we have the  $\text{F}_{\text{II}}\text{D}_{\text{II}}$  conformation and in vacuo the computed one is  $\text{F}_{\text{I}}\text{D}_{\text{II}}$ , whereas in the solid state the most stable one is  $\text{F}_{\text{III}}\text{D}_{\text{II}}$ .

This seems to confirm that the Phe moiety has an intrinsic conformational flexibility, a feature that was originally pointed out in our first work.<sup>10</sup> The best way to look for the "biologically active conformation" is probably to identify all possible accessible conformations of comparable energy and then select one (or a few) compatible with the receptor model. We have addressed this search by means of a 120-ps molecular dynamics simulation in vacuo of  $\alpha\text{-APM}$ . The details of this calculation are described in the Experimental Section, but it is possible to summarize the main results in a fashion that amounts to a description of the conformational preferences of aspartame. The results cannot give the relative population of each conformation, since the simulation is not long enough to guarantee the equilibration with respect to the exchange between different conformations, but they show that the molecule has a very large overall flexibility.

Figure 7 shows the intervals of the distribution functions for all relevant torsional variables; arrows indicate the values where maxima were found in the distribution functions. In the case of  $\psi_1$ ,  $\omega$ ,  $\chi_{12}$ , and  $\chi_{22}$ , the distribution function has a single maximum, corresponding thus to a single conformation, but the intervals of accessible values around the maxima are rather large. In the case of  $\phi_2$  the large range of accessible values is uniformly populated, with only two very small maxima at  $-120^\circ$  and  $-70^\circ$ . The presence of two distinct ranges of values is more evident for  $\psi_2$  (one centered at  $-40^\circ$  and the other at  $150^\circ$ ) and  $\chi_{11}$  (at  $-60^\circ$  and at  $40^\circ$ ). It is possible, however, that the absence of values around  $180^\circ$  for  $\chi_{11}$  may only be due to the difficulty, in a short simulation, of overcoming the barrier connected with the strong electrostatic interaction between the  $\beta\text{-COO}^-$  and the  $\alpha\text{-NH}_3^+$  of Asp, an interaction that is profoundly modified inside the receptor.

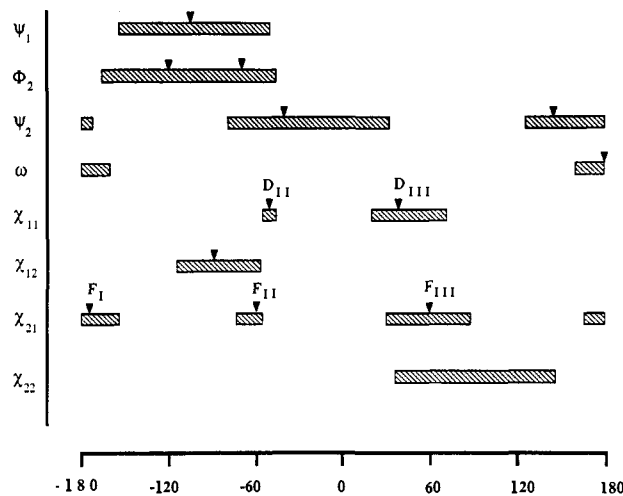


**Figure 7.** Intervals of the distribution functions for all relevant torsional variables of aspartame, as derived from a 120-ps molecular dynamics simulation in vacuo. Arrows indicate the values where maxima were found in the distribution functions.

Finally, it is most interesting that for  $\chi_{21}$  the simulation shows three fairly sharp maxima, centered at  $-60^\circ$ ,  $60^\circ$ , and  $180^\circ$ , i.e. corresponding to the three staggered conformations. This finding, although not sufficient to discriminate among the three different conformations found in different media, supports the model used to interpret the NMR data,<sup>10</sup> based on the three staggered conformers of the side chain of Phe.

As a whole, the molecular dynamics simulation shows that the backbone conformation of aspartame is not completely random, since there are definite ranges of accessible values for the rotation angles, but the width of these ranges is large enough to allow ample fluctuations around the preferred values. Besides, all the classical minima characteristic of ethanic fragments (i.e.  $g$ ,  $g^+$ , and  $t$ ) are populated for the side chains; accordingly it is not possible to pinpoint a single minimum-energy conformation among the several ones in dynamic equilibrium.

## Conclusion

The present investigation shows that it is possible to refine the model previously proposed<sup>5</sup> for the receptor site without any recourse to flexible molecules as molecular molds.

The conformation of aspartame consistent with the refined receptor model does not correspond to the most populated solution conformation, but is still one of the quasi-isoenergetic conformations in dynamic equilibrium that characterize the solution state.

## Experimental Section

**Materials. Synthesis of (2S,3S)-[ $^2\text{H}$ ]Aspartame.** (*Z*)- $\alpha$ -Acetamidocinnamic acid (Aldrich, Milwaukee, WI) was used as the starting material. Owing to the crucial importance of its configuration, we checked it by means of a NOE experiment. Irradiation of the NH proton at 9.5 ppm induced intensity changes (NOE) only in the doublet of the 2,6 protons of the aromatic ring (7.6 ppm), confirming the *Z* configuration, since in the *E* configuration only a NOE on the olefinic proton might have been expected.

1. **Deuteration of  $\alpha$ -Acetamidocinnamic Acid.** (*Z*)- $\alpha$ -Acetamidocinnamic acid (10 g) was dissolved in methanol-*d* (30 mL), and 5% Pd/C (500 mg) was added. The above mixture was deuterated with shaking at 30 psi in a Parr apparatus. After 2 days HPLC indicated complete reduction, but the mixture was allowed to react with deuterium for an additional day. At this time the solution was filtered to remove catalyst, evaporated to an oil, and crystallized from petroleum ether. The product (9.94 g, 99%) was identical with authentic *N*-acetylphenylalanine as

judged by HPLC and  $^1\text{H}$  NMR. NMR indicated 84% deuteration.

**2. Resolution of (2*RS*,3*RS*)-[ $^2\text{H}$ ]-*N*-Acetylphenylalanine.** (2*RS*,3*RS*)-[ $^2\text{H}$ ]-*N*-acetylphenylalanine (9.9 g, 0.05 mol) was dissolved in water (500 mL), the pH was adjusted to 8 with lithium hydroxide, and mold acylase I (300 mg) was added. After 72 h, during which time several adjustments of pH were required, the pH was adjusted to 5 with HCl, Norit (5 g) was added, and the mixture was filtered and concentrated and the product crystallized on addition of ethanol. The product (1.89 g, 50%) had an  $[\alpha]_{\text{D}}^{25} = -30.6^\circ$  (*c* 2,  $\text{H}_2\text{O}$ ) [authentic *L*-phenylalanine,  $[\alpha]_{\text{D}}^{25} = -34.5^\circ$  (*c* 2,  $\text{H}_2\text{O}$ )].

**3. Synthesis of (2*S*,3*S*)-[ $^2\text{H}$ ]-*N*- $\alpha$ -(Benzyloxycarbonyl)- $\beta$ -benzyl-*L*-aspartylphenylalanine Methyl Ester.** The methyl ester of (2*S*,3*S*)-[ $^2\text{H}$ ]phenylalanine was prepared in 43% yield with thionyl chloride in methanol (*R<sub>f</sub>* 0.68 butanol/acetic acid/water/pyridine 15:3:12:10). This material (0.7 g, 3.5 mmol) and *N*-methylmorpholine (0.39 mL, 3.6 mmol) in dimethylformamide were added to the mixed anhydride formed from *N*- $\alpha$ -(benzyloxycarbonyl)- $\beta$ -benzyl-*L*-aspartic acid (1.5 g, 4.2 mmol) and isobutyl chloroformate (0.53 mL, 4.1 mmol) in tetrahydrofuran (10 mL) at  $-15^\circ\text{C}$  in the presence of *N*-methylmorpholine (0.53 mL, 4.1 mmol). The protected dipeptide was isolated by standard procedures and crystallized from ethyl ether; yield 1.36 g (68%). The product was homogeneous on silica thin layers (*R<sub>f</sub>* 0.25 butanol/acetic acid/water/pyridine 15:3:12:10; *R<sub>f</sub>* 0.85 butanol/ammonium hydroxide/ethanol 40:5:5) and gave one peak on reversed-phase HPLC using a  $\text{C}_{18}$  column and an acetonitrile/water/TFA gradient from 45 to 55% acetonitrile (0.025% TFA). Proton NMR indicated the correct product.

**4. (2*S*,3*S*)-[ $^2\text{H}$ ]Phenylalanylaspargame.** The protecting groups from (2*S*,3*S*)-[ $^2\text{H}$ ]-*N*- $\alpha$ -(benzyloxycarbonyl)- $\beta$ -benzyl-*L*-aspartylphenylalanine methyl ester were removed by catalytic hydrogenation in a Parr apparatus. The yield was quantitative. The product moved with authentic aspartame but exhibited an 8% impurity on HPLC with a  $\text{C}_{18}$  reversed-phase column and an acetonitrile/water/TFA gradient.

Proton NMR revealed the expected resonances and the fact that the  $\alpha$  and  $\beta$  protons of phenylalanine were deuterated.

**Materials.** DMSO- $d_6$  (99.96%  $^2\text{H}$  atom) and  $\text{CDCl}_3$  (99.98%  $^2\text{H}$  atom) were purchased from Aldrich (Milwaukee, WI).  $\text{D}_2\text{O}$  (99.98%  $^2\text{H}$  atom) and  $\text{CD}_3\text{OH}$  (99.8%  $^2\text{H}$  atom) were purchased from C. Erba, Milano, Italy.

**NMR Measurements.** Approximately 1 mM solutions were prepared in all solvent systems.  $^1\text{H}$  spectra were recorded on Bruker AC-270, AM-400, and WM-500 spectrometers.

16 or 32 K data points were used for acquisition and 32 or 64 K, respectively, for transformation. Experimental details are indicated in the figure captions.

**Molecular Dynamics Calculation.** Intramolecular energy has been evaluated, taking into account stretching ( $d$ ), bending ( $\theta$ ), and torsion contributions, both proper ( $\phi$ ) and improper ( $\tau$ ), and adding nonbonded, van der Waals and electrostatic interactions according to the equation:

$$V = \sum \frac{1}{2} K_d (d - d_0)^2 + \sum \frac{1}{2} K_\theta (\theta - \theta_0)^2 + \sum \frac{1}{2} K_\tau (\tau - \tau_0)^2 + \sum_{i>j} V_0 [1 + \cos(n\phi - \theta)] + \sum_{i>j} \left( \frac{A}{r_{ij}^{12}} - \frac{B}{r_{ij}^6} + \frac{q_i q_j}{r_{ij}} \epsilon \right)$$

Hydrogen-bond contributions have been calculated according to the suggestion of Hagler et al.,<sup>29</sup> whereas  $A$ ,  $B$ ,  $q_i$ , and  $q_j$  have been chosen according to ref 30. Molecular dynamics (MD) simulations have been performed in the NVT (i.e. constant number, volume, and temperature of particles) ensemble, taking into account the coupling of the system to a thermal bath<sup>31</sup> at 300 K with a time constant of 0.01 ps. Before starting the MD simulation, we have performed an energy minimization using a geometry derived from a solid state study<sup>12</sup> and using the solid-state conformation ( $F_{\text{MD}}$ ) as a starting point. After minimization, in order to relax the structure to the force field used, randomly chosen velocities have been assigned to each particle according to a Boltzmann distribution. Overall molecular rotations and translations have been then stopped and 2 ps of MD were run to thermally equilibrate the system.

The time constant was then reset to 0.1 ps and the MD simulation started. Owing to the small dimensions of the molecule, a very large cut-off distance (20 Å) has been assumed both for van der Waals and electrostatic interactions. In fact, in the case of small molecules, the use of a shorter cut-off distance may lead to large fluctuations of the potential energy due to great changes in the number of nonbonded contacts upon changing the molecular conformation.

For the integration algorithm of the Newton equations, a simple leap-frog procedure was employed in connection with the constraint of the bond lengths by means of the SHAKE algorithm.<sup>32,33</sup> This allows a large integration step (0.002 ps) since the fast stretching components of the motion are now constrained. The simulation has been performed by using the GROMOS package of programs.

**Acknowledgment.** We are indebted to Dr. W. F. van Gunsteren, University of Gröningen, Holland, who kindly provided a copy of his GROMOS package of programs. Support of Grant GM 22086 from the National Institutes of Health is gratefully appreciated.

**Registry No.** SNN, 123640-84-6; TSN, 123640-85-7; aspartame, 22839-47-0; (*Z*)- $\alpha$ -acetamidocinnamic acid, 55065-02-6; (2*RS*,3*RS*)-[ $^2\text{H}$ ]-*N*-acetylphenylalanine, 75671-32-8; (2*S*,3*S*)-[ $^2\text{H}$ ]-*N*- $\alpha$ -(benzyloxycarbonyl)- $\beta$ -benzyl-*L*-aspartylphenylalanine methyl ester, 123640-86-8; (2*S*,3*S*)-[ $^2\text{H}$ ]phenylalanine methyl ester, 123640-87-9; mixed anhydride from *N*- $\alpha$ -(benzyloxycarbonyl)- $\beta$ -benzyl-*L*-aspartic acid and isobutyl chloroformate, 123640-88-0; *N*- $\alpha$ -(benzyloxycarbonyl)- $\beta$ -benzyl-*L*-aspartic acid, 3479-47-8; (2*S*,3*S*)-[ $^2\text{H}$ ]phenylalanylaspargame, 123640-89-1.

- (29) Hagler, A. T.; Huler, E.; Lifson, S. *J. Am. Chem. Soc.* **1974**, *96*, 5319-5326.
- (30) Hermans, J.; Berendsen, H. J. C.; van Gunsteren, W. F.; Postma, J. P. *Biopolymers* **1984**, *23*, 1513-1518.
- (31) Berendsen, H. J. C.; Postma, J. P.; van Gunsteren, W. F.; Di Nola, A.; Haak, J. R. *J. Chem. Phys.* **1984**, *81*, 3684-3690.
- (32) Ryckaert, J. P.; Ciccolti, G.; Berendsen, H. J. C. *J. Comput. Phys.* **1977**, *23*, 327-335.
- (33) van Gunsteren, W. F.; Berendsen, H. J. C. *Mol. Phys.* **1977**, *34*, 1311-1327.